Multi-Scale Mapping of Diaphyseal Stresses Across Gait Modalities Using Femoral Digital Twins

Mikayla R. Hoyle[a], Saulo Martelli[b], Marcus G. Pandy[c], Mariana E. Kersh[a,d,e,*]

[a] *Department of Mechanical Science and Engineering; University of Illinois Urbana-Champaign, Urbana, IL, USA*
[b] *Department of Biomedical Engineering and Biomechanics; Queensland University of Technology, Brisbane City, QLD, Australia*
[c] *Department of Mechanical Engineering, Brisbane City, QLD, Australia; University of Melbourne, Parkville, VIC, Australia*
[d] *Beckman Institute for Advanced Science and Technology; University of Illinois Urbana-Champaign*
[e] *Carle Illinois College of Medicine; University of Illinois Urbana-Champaign*

Abstract

Bone health decreases with age and can culminate in fractures with particularly devastating consequences in the femur. Exercise-induced mechanical loading can be prescribed as preventative care, but clinical recommendations are hindered by a lack of clarity regarding the mechanical stresses experienced during habitual locomotive tasks such as walking, stair descent, and stair ascent. We used subject-specific, muscle-driven finite element *digital twins* of post-menopausal women to conduct a multi-scale analysis of the spatiotemporal distribution of femoral principal stresses during each task. At the macroscopic level, stresses peaked during both the early and late stance phases of the gait cycle and the femur was subjected to a combination of bending and torsional loads for all tasks. Mesoscale analyses revealed a noticeable regional partition: stress distributions were highly consistent across tasks and timepoints in the proximal and mid-diaphysis, but deviated in the distal diaphysis. At the tissue level, peak stresses during stair ascent were lower in the proximal region but higher in the distal region compared to walking and stair descent; meanwhile, in the mid-diaphysis, peak stresses during stair descent exceeded those during walking. Together, these findings indicate that while the global femoral loading environments were similar across tasks, there was heterogeneity in the spatial and temporal mechanical response. Incorporating stair activity into daily routines can diversify bone remodeling stimulation throughout the diaphysis.

Keywords: Bone, Stress, Exercise, Walking, Stair use, Femur, Finite element

1. Introduction

Maintaining bone health is essential for quality of life and becomes particularly salient with aging when the risk of fracture increases [1]. Mechanical loading is critical for bone quality with the potential for stimulating bone adaptation as described by Frost's mechanostat theory [2]. There are numerous examples demonstrating the net formative response of bone to increased [3–5] mechanical stimulation beyond habitual activity.

In human adults, the use of walking as a form of exercise-based stimuli for bone, has produced modest positive adaptations dependent on the distance walked per week [6, 7]. When comparing individuals who walk regularly to those with a sedentary lifestyle, regular walking lowers hip fracture incidence [8]. Coupling walking with other exercise can further increase bone adapta-

*Corresponding author
Email address: mkersh@illinois.edu (Mariana E. Kersh)

tion [9]. Thus, while the evidence basis supporting the use of exercise for bone health is emerging, it would be bolstered by a clearer understanding of the homeostatic range of mechanical stimuli bone is subjected to during habitual locomotion.

There are several experimental and modeling methods for estimating bone stresses. Experimentally, *in vitro* measurements of femoral strains have been reported by loading a subset of muscles attached to the femur [10]. While valuable, these experiments are limited to surface strain measurements. Alternatively, rigid body modeling [11] can provide line element results, but neglect the geometric complexity of bone. Partially subject-specific, muscle-driven finite element (FE) models have reported von Mises stress in the femoral diaphysis during walking [12, 13]. Von Mises stress is useful for inferring bone strength relative to yielding. However, an assessment of habitual loads using principal stresses affords insight into both the magnitude and type of loads (i.e, tensile vs compressive loads). To our knowledge, the principal stresses in the femoral diaphysis during habitual locomotive tasks (walking and stair use) have not been reported using subject-specific, muscle-driven FE models.

In addition to informing the development of exercise-based protocols for bone health, characterizing the stresses in the femoral diaphysis has relevance in several clinical applications. For example, in runners, the femoral diaphysis is a common location for fatigue initiated stress injuries [14]. The biomechanical mechanisms underlying the rare, but troubling, atypical fractures following bisphosphonate use in those with osteoporosis [15–17] remain unclear given that the fractures happens in regions of thick cortical bone and without trauma [18].

Therefore, the aim of this study was to assess the bulk macroscopic loading and tissue-level stress-state of the femoral diaphysis during walking, stair ascent, and stair descent. We performed a multi-scale analysis using subject-specific, muscle-driven digital twins of healthy post-menopausal women to assess the spatiotemporal evolution of stresses during the stance phases of these common locomotive tasks. Quantifying the *in vivo* stresses during habitual locomotive tasks would elucidate the homeostatic mechanical stimuli relevant to the design of exercise interventions as well as clinical scenarios involving diaphyseal fractures.

2. Methods

2.1. Subjects

The absolute maximum principal stresses in the femoral diaphysis during walking, stair ascent, and stair descent were analyzed using previously developed [19], subject-specific, muscle-driven FE models of postmenopausal women (n=18, age range: 60 to 74 years) with no history of bone disease. Unrecoverable errors in data collection prevented analyses of one subject's stair usage data resulting in n=17 models for both stair ascent and stair descent. The stance phase of each task was discretized into 20 timepoints and normalized between 0 and 100%. These data were further separated into five intervals: heel strike ($0-20\%$), early stance ($21-40\%$), mid stance ($41-70\%$), late stance ($71-85\%$), and toe off ($86-100\%$).

2.2. Model registration

The diaphysis was defined as the region spanning from the lesser trochanter (identified within the computed tomography-based computer-aided design models) to 120 mm above the proximal end of the condyles. Elements corresponding to bone marrow (Young's modulus, $E < 2500\,MPa$) were removed, and all models were co-registered using the linea aspera within the distal diaphysis (Python 3.12.7). For each task, the absolute maximum principal stresses (herein referred to as principal stress) during the stance phase were calculated.

2.3. Whole-bone macroscopic analysis

To visually characterize the bulk deformation of the femur during locomotion, the displacements were scaled by a factor of 15. The resulting visualizations were used to assess the loading of the femur in the frontal and sagittal anatomical planes.

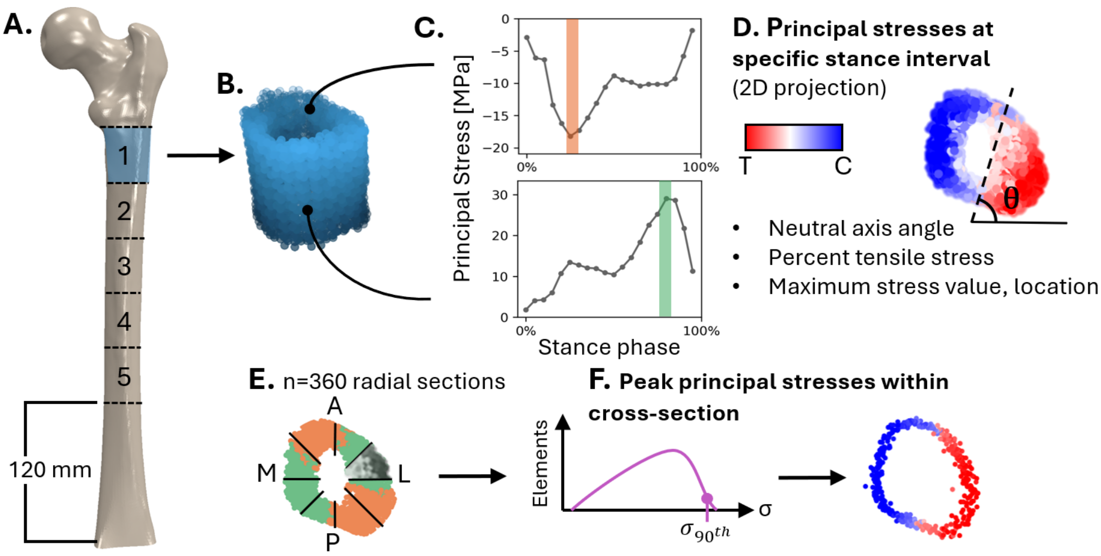

Figure 1: Data processing of (A) five equidistant sections of the femoral diaphysis. (B,C) The highest principal stresses and corresponding timing during stance was identified. (D) Principal stresses during the times of maximum stress was analyzed using 2D projections. (E,F) The 90th percentile principal stress within each radial section was also calculated. Figure is of a representative subject.

2.4. Meso-scale analysis during discrete stance intervals

We characterized the meso-scale stress state of the femur by dividing the diaphysis into five equidistant sections (Fig.1A) and first assessing *when* the stress was maximum within each section. For each element, we identified the stance interval corresponding to when principal stress was highest during stance (Fig.1B,C). We then calculated the proportion of each section under maximum stress during each stance interval. Initial analyses revealed that peak stresses occurred during early and late stance for walking and stair descent, and early stance for stair ascent (Table 1, Fig.2A). Thus, the meso-scale stress-state was characterized during these two timepoints for all activities.

The element centroids of each diaphyseal section were projected onto 2D cross-sections (Fig. 1D) and used to plot the principal stresses during early and late stance. From these graphs, we measured the neutral axis orientation with respect to the medial-lateral axis ($0 - 180°$, ImageJ 1.52p), the percent of each cross-section under tension, and the maximum tensile and compressive principal stresses (Fig. 1D).

While in theory the neutral axis can be measured as between $0 - 180°$, interpretation of this data is dependent on whether the change in neutral axis is a result of bending or torsion. To account for this, continuous changes in the orientation of the neutral axis (relative to the adjacent section) due to torsion were adjusted to beyond 180°.

2.5. Tissue-level peak stress analysis

To compare the peak principal stresses between tasks (independent of stance time), each projected cross-section was divided into 360 radial sections. (Fig. 1E). For each radial section, the 90th percentile principal stress was calculated and visualized at the geometric centroid of each radial section (Fig.1F). The peak principal stress data were filtered using a low-pass Butterworth filter as a function of radial location.

2.6. Statistical analysis

Normality of the neutral axis measurements and the percent of the projected cross-section under tensile loads were confirmed using a Shapiro-Wilk test. Both measures were analyzed using one-way repeated measures ANOVA followed by a post-hoc analysis with a paired t-test and Bonferroni correction (R Studio, Boston, MA, USA).

Table 1: Spatial distribution of peak principal stress timing across femoral diaphyseal regions. Values represent the percentage of the total cross-sectional area reaching peak stress during each stance interval.

Diaphysis	Walking					Stair descent					Stair ascent				
section	HS	ES	MS	LS	TO	HS	ES	MS	LS	TO	HS	ES	MS	LS	TO
Prox: S1	-	45.0	-	55.0	-	-	72.5	-	27.5	-	-	97.5	-	-	2.5
S2	-	37.5	-	62.5	-	-	77.5	-	22.5	-	-	100.0	-	-	-
S3	-	34.2	-	65.8	-	-	71.9	-	28.1	-	0.8	99.2	-	-	-
S4	-	73.3	-	26.7	-	0.3	93.6	-	6.1	-	-	100.0	-	-	-
Dist: S5	2.2	74.7	-	23.1	-	1.9	64.2	-	33.9	-	-	100.0	-	-	-

HS = Heel Strike; ES = Early Stance; MS = Mid Stance; LS = Late Stance; TO = Toe Off.

Stance phase stresses were not normally distributed (D'Agostino-Pearson K2) and comparisons between locomotions were performed using Statistical non-Parametric Mapping (SnPM; spm1d v.0.4.18) with one-way ANOVA [20]. Post-hoc analysis was performed with a two-sample t-test and Bonferroni correction. In significant regions, the average percent difference of the peak stress magnitude was calculated. When the peak stress direction differed in significant regions, SnPM was performed on the magnitudes to confirm significance. Significance was set at $\alpha = 0.05$.

3. Results

3.1. Timing of peak stress

During walking and stair descent, the peak stresses most commonly occurred during early and late stance, while the peak stresses during stair ascent occurred only during early stance (Table 1). Across all three tasks, peak stresses occurred at 25.3±4.0% and 75.5±1.6% of the stance phase of gait.

3.2. Macroscopic deformation

All three locomotive tasks exhibited similar macroscopic deformations. During early stance, the femur was under lateral S-shape bending (frontal), internal torsional rotation (frontal), and posterior cantilever bending (sagittal)(Fig 2A). Late stance resulted in medial S-shaped bending and a tendency towards anterior buckling. (Fig 2B).

3.3. Stress distributions during early and late stance

Our qualitative observations of the macroscopic deformations of the femoral diaphysis were confirmed by the quantitative tissue-level analyses of stresses. Specifically, there was a clear distinction in stress distributions between the proximal/mid diaphyseal regions (S1-S3) and the distal diaphysis (S4-S5, Fig.3A).

Proximal and mid-diaphysis (S1-S3): the neutral axis was aligned with the anterior-posterior axis ($81.3 \pm 15.0°$, Fig.3A dashed lines, Fig.3B). There was a modest medial rotation of the neutral axis at the mid-diaphysis ($\Delta 12.6°$, $p = 0.026$ to < 0.001) during the early stance phase of stair ascent. In contrast, the neutral axis orientation was relatively constant during the late stance phase of all three locomotive tasks with the exception of stair descent (S1-S2: $p = 0.018$).

In all tasks, the lateral half of the proximal diaphyseal sections were in tension during both early and late stance (S1,S2: 45.1±3.5%; Fig.3A red regions; Fig.3C). The percent of each cross-section in tension decreased by 19.0% in the mid diaphysis ($p < 0.001$). The stresses were highest in the most proximal section (S1), and the maximum compressive stress was 23% higher than the maximum tensile stress (C: $-27.0\,MPa$, T: $21.5\,MPa$; Fig.3D). In the subsequent two sections (S2 and S3), the maximum stress values decreased by 24% relative to the most proximal section.

Lower-middle diaphysis (S4): Compared to the mid-diaphysis, torsion during the early stance phase of walking and stair ascent resulted in a pronounced medial rotation of the neutral axis in the lower-middle diaphysis ($\Delta 78.0°$; $p < 0.001$; Fig.3A,B). A less pronounced rotation occurred during the late stance phase of stair activity ($\Delta 34.8°$; $p = 0.02$, $p = 0.008$). Additionally, the percent under tension decreased by 18.09% for all tasks ($p = 0.002$ to $p < 0.001$) except for the early stance phase of stair ascent. Compared to all other sections, the stresses in the lower-middle diaphysis were the lowest (C: $-10.7\,MPa$, T: $3.7\,MPa$).

Distal diaphysis (S5): Compared to the lower-middle diaphysis, the neutral axis during the early stance phase of stair ascent continued to rotate medially from the torsional load ($\Delta 16.1°$; $p < 0.001$). In contrast, the neutral axis rotated by 26.4° laterally during the late stance phase of stair ascent and the medial aspect was under tension. For the early stance phase of stair descent and the late stance of the other tasks, the neutral axis angle did not rotate but instead shifted medially. The medial aspect was in tension as a result of the macroscopic bending inflection point. During the early phase stance of walking and stair descent, the amount of the cross-section in tension increased by 19.7%. The maximum stress values in section 5 were similar to the mid-diaphysis (C: $-13.9\,MPa$, T: $8.2\,MPa$). We note that for early stance of stair descent and the late stance of all tasks, the stress state (bending with a neutral axis oriented along the anterior-poster direction) in the distal diaphysis (S5) is nearly equal to the mid-diaphysis (S3) with the primary difference being the location of the region under tension.

3.4. Peak local stresses due to locomotion

Our last analysis involved local comparisons of peak stresses within each femoral cross-section between the different tasks. In general, peak stresses during walking and stair descent were similar. Compared to walking and stair descent, the stresses during stair ascent were lower in the proximal diaphysis and higher in the distal diaphysis.

Within the two most proximal regions, stair ascent resulted in lower stresses in the anterolateral and posteromedial quadrants. (Fig4A,B). In the most proximal region (S1), the stresses during stair ascent were $79.4 \pm 32.5\%$ lower than those during walking and stair descent ($p = 0.012$). In S2, stresses were $49.3 \pm 13.6\%$ lower than the stresses during walking and stair descent (< 0.001). In the mid-diaphysis, the peak stresses on the posterior aspect during walking were $53.8 \pm 13.8\%$ lower than the stresses during stair descent ($p = 0.016$; Fig4C).

In the distal regions, the loading mode during stair ascent shifted from compression to tension in the anterior quadrants (Fig4D,E). Upon comparing the magnitudes, there was only a small lateral region in section 5 where the stresses during stair descent were higher than the stresses during stair ascent. In the posterior regions, the peak stresses for all tasks were compressive. In sections 4, the stresses during stair ascent were $23.7 \pm 18.33\%$ higher than walking and stair descent ($p < 0.001$), and in section 5 they were $70.1 \pm 30.5\%$ higher ($p = 0.002$).

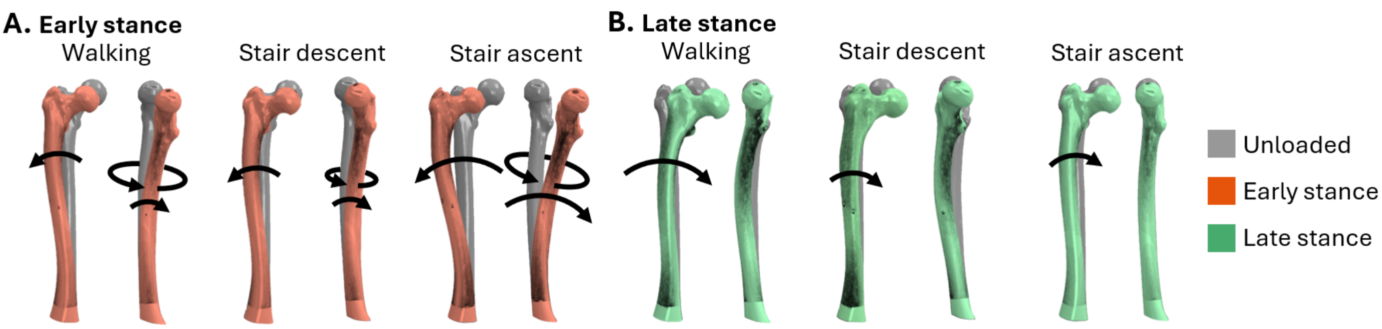

Figure 2: Whole bone, macroscopic, load condition in the frontal (left) and sagittal (right) views for each task during (A) early and (B) late stance. This figure is of a representative subject.

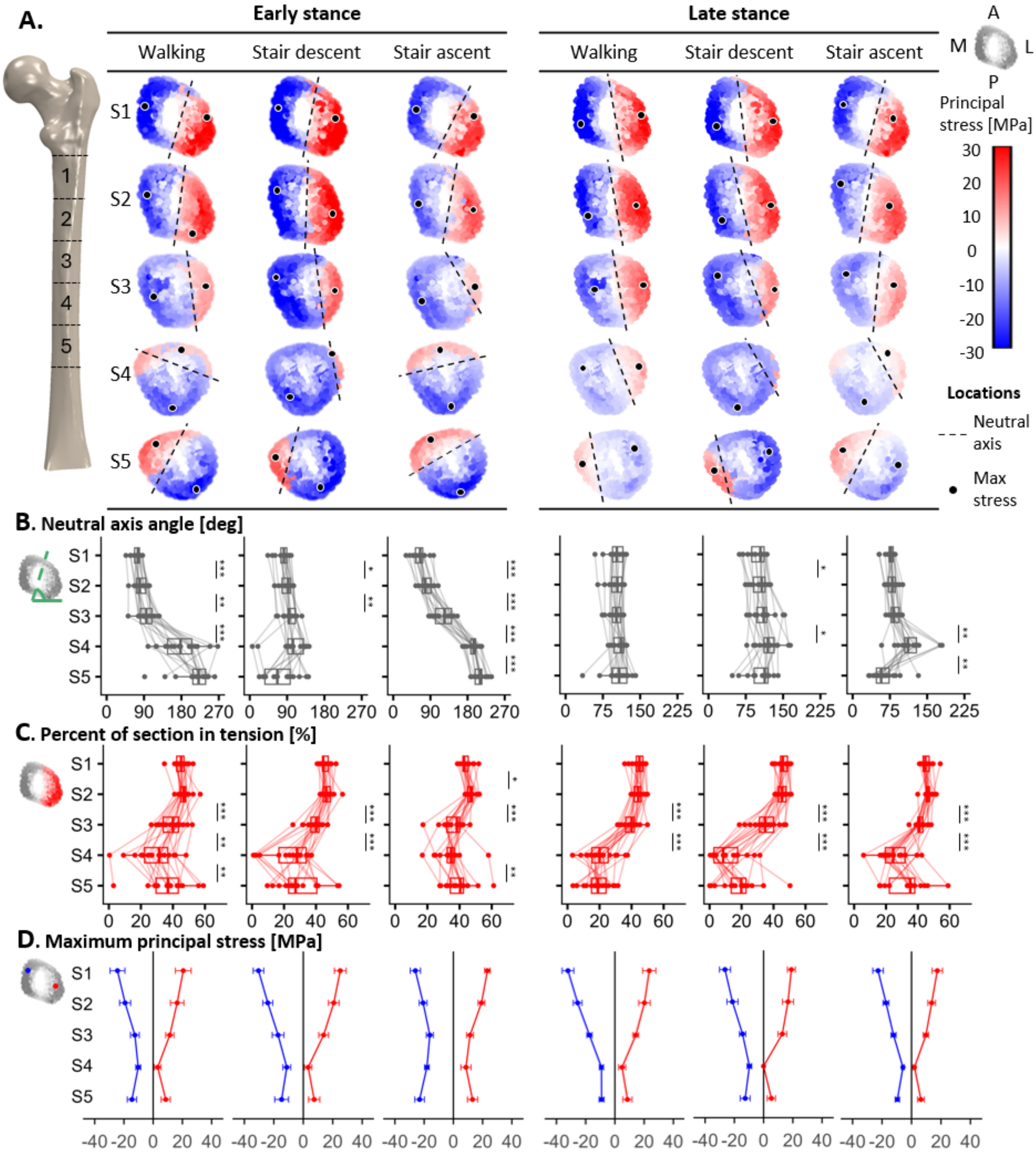

Figure 3: (A) Principal stress distribution for each task during early stance and late stance. (B) Neutral axis orientation. (C) Portion of each section under tensile stress. (D) Maximum principal compressive and tensile stress. * $p < 0.05$ ** $p < 0.01$ *** $p < 0.001$

4. Discussion

Spatiotemporal variations in diaphyseal stresses were observed during habitual locomotion using subject-specific, muscle-driven femoral digital twins of healthy post-menopausal women. While this framework has been used to characterize the mechanical environment within the femoral neck and trochanteric region [19, 21], to our knowledge the current study provides the first comprehensive mapping of tensile and compressive principal stresses throughout the femoral diaphysis during these tasks. Overall, stresses

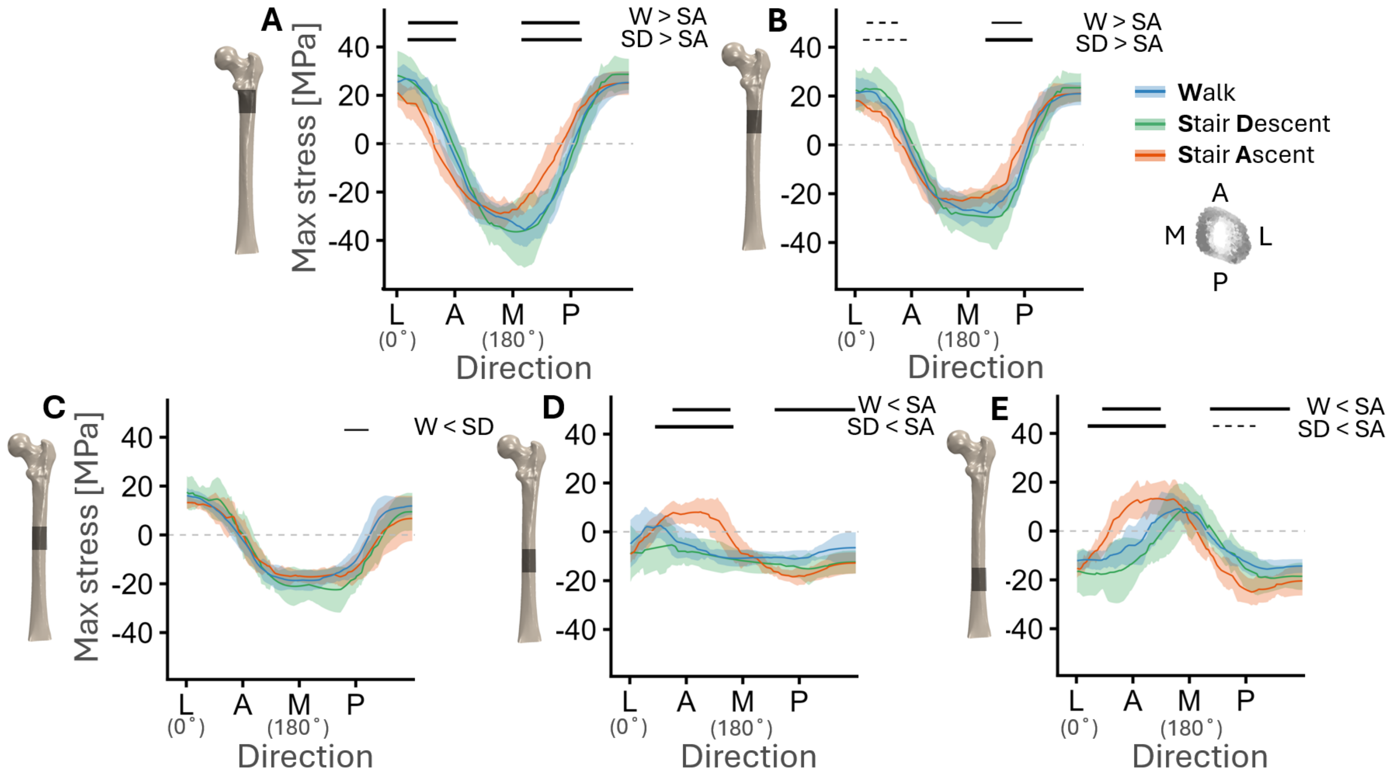

Figure 4: SnPM results for stresses in each (A-E) vertical section during all three locomotions. Solid lines indicate the mean, and shaded regions represent the standard deviation. (W, walking; SA, stair ascent; SD, stair descent) $p < 0.05$ $p < 0.01$ $p < 0.001$

were highest within the proximal diaphysis, with peak magnitudes occurring during early and late stance. The peak stresses throughout the diaphysis were similar between walking and stair descent, but differed during stair ascent, reflecting shifts in the multi-axial loading regimes between tasks.

While others have reported principal stresses during locomotion, there is no quantitative data that allows for a direct model-to-model comparison [22–25]. However, qualitatively the spatial distribution of principal stresses reported in these studies are similar to our own distributions. Spiers et al. assessed principal strains during walking and stair ascent, finding spatial distributions consistent with our study [26]. Specifically, they found that the principal strains during stair ascent in the proximal diaphysis were lower than walking, while in the distal diaphysis strains during stair ascent were higher which is in agreement with our results. In contrast to our finding that stair descent results in lower stresses in the distal diaphysis compared to stair ascent, Deng et al reported consistently higher principal strains during stair descent compared to stair ascent throughout the diaphysis[27]. The use of a single femoral geometry and associated material properties for their analyses, in contrast to our subject-specific models, may contribute to the observed differences. Finally, Polgar et al. analyzed the orientation of the neutral axis during heel strike of walking based on principal strains and are similar (within one standard deviation) to our measurements of the neutral axis orientation during early stance [28].

We found that the peak principal stresses during walking and stair descent were similar in the diaphysis. Both walking and stair descent gait patterns can be characterized as a controlled series of forward falling and recovery, with stair descent having a farther distance to fall. In contrast, stair ascent requires a pushing action early in the stance phase to enable upward movement to the next step. As expected, these two gait styles require different muscles and is most clearly seen in the gluteus maximus force profiles[19]. During stair ascent, gluteus maximus force was approximately double that of the force during walking and stair descent. Curiously, despite this increase in muscle force, principal stresses in the proximal diaphysis were lower during stair ascent suggesting that either co-contraction of opposing muscles (or the hip joint reaction force vector) may offset the effects of increased gluteus medius. Given that the principal stresses in the femur are a result of over twenty temporally and spatially varying muscle forces culminating in a complex, multimodal stress-state there is a desire for proxy measurements of the local mechanical environment. Using the ground reaction force as a proxy for the femoral diaphysis stress-state may not provide enough information. For example, during stair ascent, the GRF was higher during late stance [19], but our results show the diaphyseal stresses were exclusively higher during early stance. Similar conclusions have also been made regarding the femoral neck and tibia [19, 29].

None-the-less, the stresses were consistently higher in the proximal diaphysis, nearest to the hip joint reaction force and most of the muscle insertion points. The three highest muscle forces - gluteus medius, gluteus maximus, and iliopsoas [19] - insert into the greater trochanter, proximal diaphysis, and lesser trochanter, respectively. This high-stress region corresponds to where half of reported atypical femoral fractures (AFF) occur [30], as well as where femoral stress injuries are found in runners [14]. Interestingly, these two fracture types most commonly occur in different anatomical quadrants. An AFF typically begins on the lateral aspect (where the tensile stresses were concentrated) and perpetuates as a stress fracture due to fatigue [18]. The combination of bone being mechanically weaker in tension [31] and the lack of remodeling from bisphosphonates could be a potential mechanism driving AFFs. Stress injuries in athletes most commonly occur on the medial aspect [14] - a region we found to be in compression. We attribute the tensile versus compressive distributions to longitudinal bending of the femur as a result of the muscle insertion locations relative to the joint reaction force. However, whole bone geometry, including the bicondylar angle of the femur, may also contribute to femoral bending [32–36]. More work is needed to understand the relative contribution of femoral geometry and muscle forces to the meso- and tissue level stress state during locomotion.

The current study has several strengths, including being the first to report tensile and compressive principal stresses for the entire diaphysis during three habitual locomotive tasks using a complete subject-specific, muscle-driven finite element model of healthy post-menopausal women. However, this study also has several limitations. Our study is limited to one specific population. Locomotion style, and therefore muscle forces, may differ by age and sex [37, 38]. Our models used an isotropic Young's moduli. While an orthotropic Young's moduli would be more accurate, the resulting stresses when using isotropic or orthotropic material properties have been found to be only marginally different [39]. The use of a fixed boundary condition at the distal diaphysis may result in an overestimation of stresses. However, our regions of interest followed and exceeded Saint-Venant's principle and were applied systematically to all models. For this reason, we did not include the gastrocnemius muscles as they overlap spatially with our fixed constraints [40]. Future studies could extend this framework to other activities, such as running, that cause higher bone loads and are more likely to stimulate bone adaptation [41, 42].

Overall, our results reveal that diaphyseal loading is similar during walking and stair descent, but distinct from stair ascent. We found spatial and temporal differences in the mechanical response of bone to the locomotive forces. Focusing on walking as the habitual activity, and incorporating stair ascent may be a viable option for bone maintenance. Our study provides an anatomical mechanical atlas to understand the normative stress state during habitual locomotive tasks and thus a foundation for future work evaluating bone quality.

5. Acknowledgments

Mikayla R. Hoyle: Writing – review & editing, Writing – original draft, Visualization, Software, Investigation, Formal analysis. Saulo Martelli: Data curation. Marcus G. Pandy: Data curation. Mariana E. Kersh: Writing – review & editing, Supervision, Resources, Project administration, Funding acquisition, Data curation, Conceptualization.

6. Conflict of Interest

Declarations of interest: none.

References

1. Kanis JA, Borgstrom F, De Laet C, Johansson H, Johnell O, Jonsson B, Oden A, Zethraeus N, Pfleger B, Khaltaev N. Assessment of fracture risk. *Osteoporosis International* 2005;16(6):581–9.

2. Frost HM. Bone "mass" and the "mechanostat": A proposal. *The Anatomical Record* 1987;219(1):1–9.

3. Warden SJ, Mantila Roosa SM, Kersh ME, Hurd AL, Fleisig GS, Pandy MG, Fuchs RK. Physical activity when young provides lifelong benefits to cortical bone size and strength in men. *Proceedings of the National Academy of Sciences* 2014;111(14):5337–42.

4. Fujii N, Imura T, Mitsutake T, Hirohama K, Okimoto N, Tsukamoto M, Tanaka R. Effects of exercise on the cortical bone of the proximal femur in women: A systematic review and meta-analysis. *Bone* 2026;203:117740.

5. Chen X, Aoki H, Fukui Y. Effect of exercise on the bone strength, bone mineral density, and metal content in rat femurs. *Bio-Medical Materials and Engineering* 2004;14(1):53–9.

6. Cummings SR, Nevitt MC, Browner WS, Stone K, Fox KM, Ensrud KE, Cauley J, Black D, Vogt TM. Risk Factors for Hip Fracture in White Women. *New England Journal of Medicine* 1995;332(12):767–73.

7. Krall EA, Dawson-Hughes B. Walking is related to bone density and rates of bone loss. *The American Journal of Medicine* 1994;96(1):20–6.

8. Landgraff IK, Meyer HE, Ranhoff AH, Holvik K, Talsnes O, Myrstad M. Resting heart rate, self-reported physical activity in middle age, and long-term risk of hip fracture. A NOREPOS cohort study of 367,386 men and women. *Bone* 2023;167:116620.

9. Palombaro KM. Effects of Walking-only Interventions on Bone Mineral Density at Various Skeletal Sites: A Meta-analysis. *Journal of Geriatric Physical Therapy* 2005;28(3):102.

10. Cristofolini L, Viceconti M, Toni A, Giunti A. Influence of thigh muscles on the axial strains in a proximal femur during early stance in gait. *Journal of Biomechanics* 1995;28(5):617–24.

11. Munih M, Kralj A, Bajd T. Bending moments in lower extremity bones for two standing postures. *Journal of Biomedical Engineering* 1992;14(4):293–302.

12. Taylor ME, Tanner KE, Freeman MAR, Yettram AL. Stress and strain distribution within the intact femur: Compression or bending? *Medical Engineering & Physics* 1996;18(2):122–31.

13. Wagner DW, Divringi K, Ozcan C, Grujicic M, Pandurangan B, Grujicic A. Combined musculoskeletal dynamics/structural finite element analysis of femur physiological loads during walking. *Multidiscipline Modeling in Materials and Structures* 2010;6(4):417–37.

14. Hwang B, Fredericson M, Chung CB, Beaulieu CF, Gold GE. MRI Findings of Femoral Diaphyseal Stress Injuries in Athletes. *American Journal of Roentgenology* 2005;185(1):166–73.

15. Wells GA, Cranney A, Peterson J, Boucher M, Shea B, Welch V, Coyle D, Tugwell P.

Alendronate for the primary and secondary prevention of osteoporotic fractures in postmenopausal women (Review). *Cochrane Database Systematic Reviews* 2008;(1):1–77.

16. Bilezikian JP. Efficacy of Bisphosphonates in Reducing Fracture Risk in Postmenopausal Osteoporosis. *The American Journal of Medicine* 2009;122(2, Supplement):S14–21.

17. Dell RM, Adams AL, Greene DF, Funahashi TT, Silverman SL, Eisemon EO, Zhou H, Burchette RJ, Ott SM. Incidence of atypical nontraumatic diaphyseal fractures of the femur. *Journal of Bone and Mineral Research* 2012;27(12):2544–50.

18. Larsen MS, Schmal H. The enigma of atypical femoral fractures: A summary of current knowledge. *EFORT open reviews* 2018;.

19. Kersh ME, Martelli S, Zebaze R, Seeman E, Pandy MG. Mechanical Loading of the Femoral Neck in Human Locomotion. *Journal of Bone and Mineral Research* 2018;33(11):1999–2006.

20. Pataky TC. One-dimensional statistical parametric mapping in Python. *Computer Methods in Biomechanics and Biomedical Engineering* 2012;15(3):295–301.

21. Rogalski MP, Martelli S, Pandy MG, Kersh ME. Role of muscle forces on strain distributions in the proximal femur. *Journal of Biomechanics* 2025;188:112743.

22. Tamvada KH. Femoral Mechanics, Mobility, and Finite Element Analysis. In: Carlson KJ, Marchi D, eds. *Reconstructing Mobility: Environmental, Behavioral, and Morphological Determinants.* Boston, MA: Springer US. ISBN 978-1-4899-7460-0; 2014:273–89.

23. Wronski S, Wit A, Tarasiuk J, Lipinski P. The impact of the parameters of the constitutive model on the distribution of strain in the femoral head. *Biomechanics and Modeling in Mechanobiology* 2023;22(2):739–59.

24. Ali Banijamali SM, Oftadeh R, Nazarian A, Goebel R, Vaziri A, Nayeb-Hashemi H. Effects of Different Loading Patterns on the Trabecular Bone Morphology of the Proximal Femur Using Adaptive Bone Remodeling. *Journal of Biomechanical Engineering* 2015;137(011011).

25. Lotz JC, Cheal EJ, Hayes WC. Stress distributions within the proximal femur during gait and falls: Implications for osteoporotic fracture. *Osteoporosis International* 1995;5(4):252–61.

26. Speirs AD, Heller MO, Duda GN, Taylor WR. Physiologically based boundary conditions in finite element modelling. *Journal of Biomechanics* 2007;40(10):2318–23.

27. Deng C, Gillette JC, Derrick TR. Finite element analysis of femoral neck strains during stair ascent and descent. *Scientific Reports* 2021;11(1):9183.

28. Polgar K, Gill HS, Viceconti M, Murray DW, O'Connor JJ. Strain distribution within the human femur due to physiological and simplified loading: Finite element analysis using the muscle standardized femur model. *Proceedings of the Institution of Mechanical Engineers, Part H: Journal of Engineering in Medicine* 2003;217(3):173–89.

29. Matijevich ES, Branscombe LM, Scott LR, Zelik KE. Ground reaction force metrics are not strongly correlated with tibial bone load when running across speeds and slopes: Implications for science, sport and wearable tech. *PLOS ONE* 2019;14(1):e0210000.

30. Bruce OL, Haider IT, Cheung AM, Tile L, Bleakney R, Scher J, Edwards WB. Femur geometry influences atypical femoral fracture location. *Osteoporosis International* 2025;36(8).

31. Li S, Demirci E, Silberschmidt VV. Variability and anisotropy of mechanical behavior of cortical bone in tension and compres-

sion. *Journal of the Mechanical Behavior of Biomedical Materials* 2013;21:109–20.

32. Kersh ME, Pandy MG, Bui QM, Jones AC, Arns CH, Knackstedt MA, Seeman E, Zebaze RM. The heterogeneity in femoral neck structure and strength. *Journal of Bone and Mineral Research* 2013;28(5):1022–8.

33. Endo D, Ogami-Takamura K, Imamura T, Saiki K, Murai K, Okamoto K, Tsurumoto T. Reduced cortical bone thickness increases stress and strain in the female femoral diaphysis analyzed by a CT-based finite element method: Implications for the anatomical background of fatigue fracture of the femur. *Bone Reports* 2020;13:100733.

34. Oh Y, Wakabayashi Y, Kurosa Y, Fujita K, Okawa A. Potential pathogenic mechanism for stress fractures of the bowed femoral shaft in the elderly: Mechanical analysis by the CT-based finite element method. *Injury* 2014;45(11):1764–71.

35. Kaku N, Hosoyama T, Shibuta Y, Kimura M, Tsumura H. Influence of femoral bowing on stress distribution of the proximal femur: A three-dimensional finite element analysis. *Journal of Orthopaedic Surgery and Research* 2023;18(1):82.

36. Shefelbine SJ, Tardieu C, Carter DR. Development of the femoral bicondylar angle in hominid bipedalism. *Bone* 2002;30(5):765–70.

37. Kerrigan DC, Todd MK, Croce UD. GENDER DIFFERENCES IN JOINT BIOMECHANICS DURING WALKING Normative Study in Young Adults. *American Journal of Physical Medicine & Rehabilitation* 1998;77(1):2.

38. Ostrosky KM, VanSwearingen JM, Burdett RG, Gee Z. A Comparison of Gait Characteristics in Young and Old Subjects. *Physical Therapy* 1994;74(7):637–44.

39. Peng L, Bai J, Zeng X, Zhou Y. Comparison of isotropic and orthotropic material property assignments on femoral finite element models under two loading conditions. *Medical Engineering & Physics* 2006;28(3):227–33.

40. Brand RA, Pedersen DR, Friederich JA. The sensitivity of muscle force predictions to changes in physiologic cross-sectional area. *Journal of Biomechanics* 1986;19(8):589–96.

41. Uchida TK, Delp S. Biomechanics of Movement: The Science of Sports, Robotics, and Rehabilitation. Cambridge: The MIT press; 2020. ISBN 978-0-262-04420-2.

42. Lane NE, Bloch DA, Jones HH, Marshall Jr WH, Wood PD, Fries JF. Long-Distance Running, Bone Density, and Osteoarthritis. *JAMA* 1986;255(9):1147–51.